

## Supplemental Figures for Integrated Heating & Sensing for PCB EWOD Chips on Digital Microfluidics Cloud Platform

Mosfera Chowdury<sup>a</sup>, Gnanesh Nagesh<sup>a</sup>, Eric Hyunsung Cho<sup>c</sup>, Qining Leo Wang<sup>c</sup>, Bhawya<sup>a</sup>, Abdulrahman Altabbaa<sup>a</sup>, Lina Rose<sup>a,b</sup>, Simon Rondeau-Gagne<sup>a,b</sup>, Chang-Jin “CJ” Kim<sup>c,d,e\*</sup>, Mohammed Jalal Ahamed<sup>a,\*</sup>

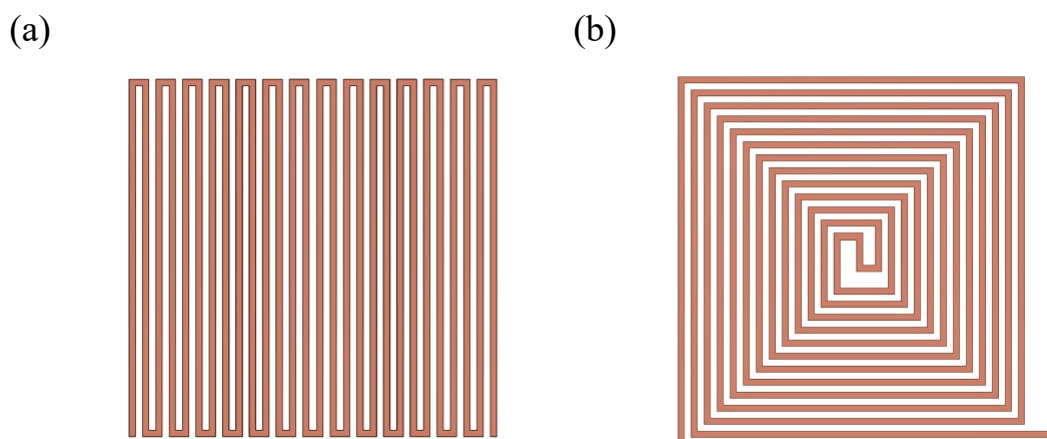


Figure S1: 2D heater design for serpentine (a) and double spiral shapes (b)



Figure S2: Four-layer PCB configuration used for manufacturing the PCB EWOD chip. Two inner copper layers are used for the heater–sensor pair.

### Hardware Design:

The DMF control system provides portability when it is used with a battery-powered electronic system (e.g., laptop, tablet). Electrically, the system provides 250 independently controlled

voltage channels, which is double the capacity of most existing systems and enables complex protocols. Safety measures, such as splitting the circuits into top and bottom plates, ensure that high voltage is inaccessible when the system is open. The C-shaped chassis is designed to accommodate DMF chips of various types, shapes, and thicknesses and is 20 cm × 8.2 cm × 2.4 cm and weighs approximately 0.4 kg.

## Microheater & Sensor Design

A serpentine-shaped thin-film microheater is designed for a copper layer, which is integrated between two FR4 prepreg layers, whereas a sensor with the same design is similarly integrated into a different copper layer, also sandwiched between prepreg layers, as depicted in Figure S2. Since the microheater and sensor were made of a copper layer within the multilayer PCB, as shown in Figure S2, their thickness was 35 μm. The line width of the heater is 150 μm, with a 150 μm gap between adjacent lines.

## Heater & Sensor Co-fabrication in a DMF Chip

The heater and sensors were placed on two copper inner layers of the 4-layer PCB. By utilizing the inner copper layers that are used for electric routing in the DMF chip, heaters and sensors for thermal management can be obtained when the DMF chip is fabricated. The serpentine-shaped heater was designed within a 2 mm × 2 mm square area on the 4-layer PCB substrate. The integrated heater footprint and PCB layout designs were designed via Altium Designer (version 24.0.1) software. This was later integrated with the design of the eDroplets DMF chip using KiCad (version 7).

The integrated serpentine heater was placed at the second copper layer, and the sensor was placed at the third copper layer of the PCB stack-up representation, as shown in Figure S2. The first (top) copper layer was used for the EWOD electrodes and contact pads, and the fourth (bottom) copper layer was used for the trace lines.

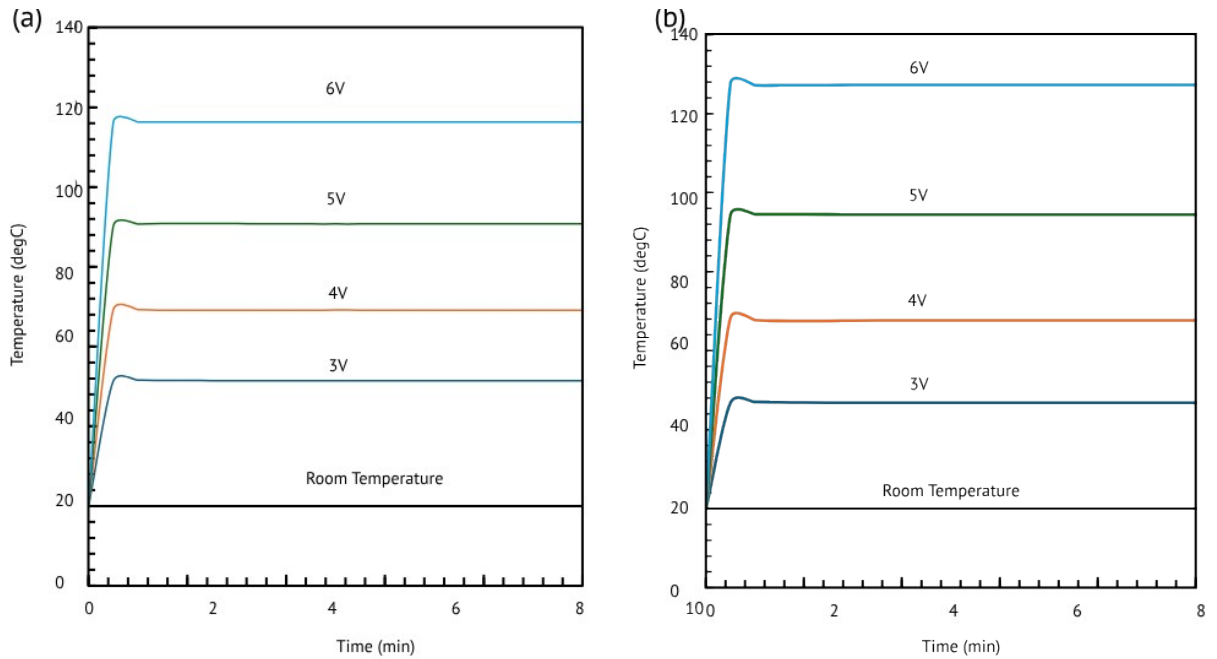


Figure S3: This figure shows the temperature variation with time at different voltages where the PCB surface arrives at a stable temperature within  $\sim 2$  min, regardless of the applied voltage for both heater designs: serpentine-shaped (a) and double spiral (b).

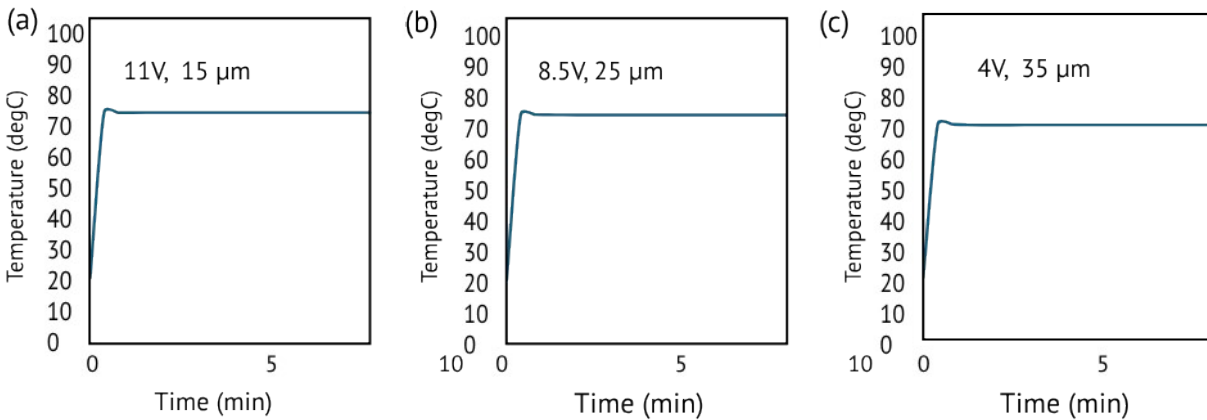
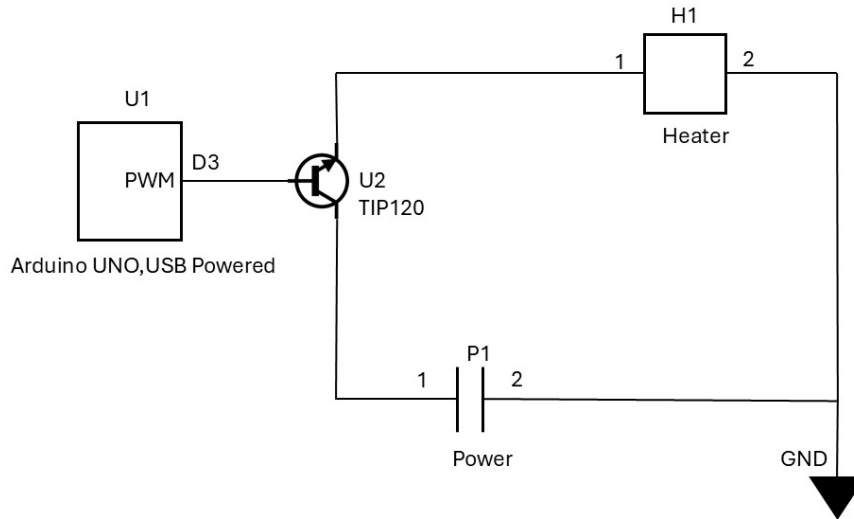


Figure S4: The temperature stability plot of the top copper surface of the PCB assembly for various serpentine microheater thicknesses shows that decreasing the microheater thickness requires a higher voltage and results in increased power consumption (a, b, and c).

(a)



(b)

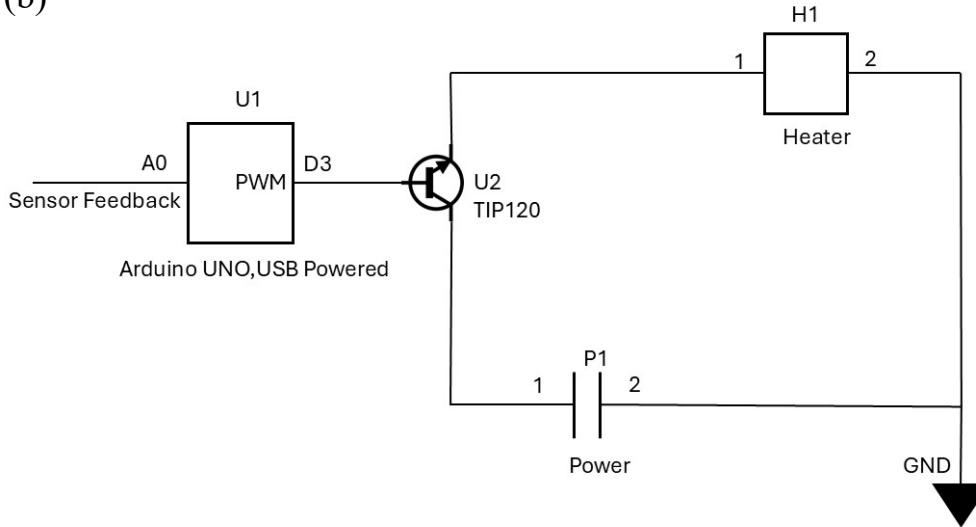


Figure S5: (a) A symbolic representation of the heater circuit (open loop). The Arduino Uno is powered by Atmega328P, which has a total of 28 pins comprising analog, digital, ground, power, and 6 pulse width modulation (PWM) pins. Here, pin D3 is used for the PWM. U2 is the transistor with the collector connected to the 5 V power P1 and the emitter connected to the heater. The base is connected to the PWM pin D3 of the microcontroller U1. (b) The closed loop configuration for the heater circuit (closed loop).

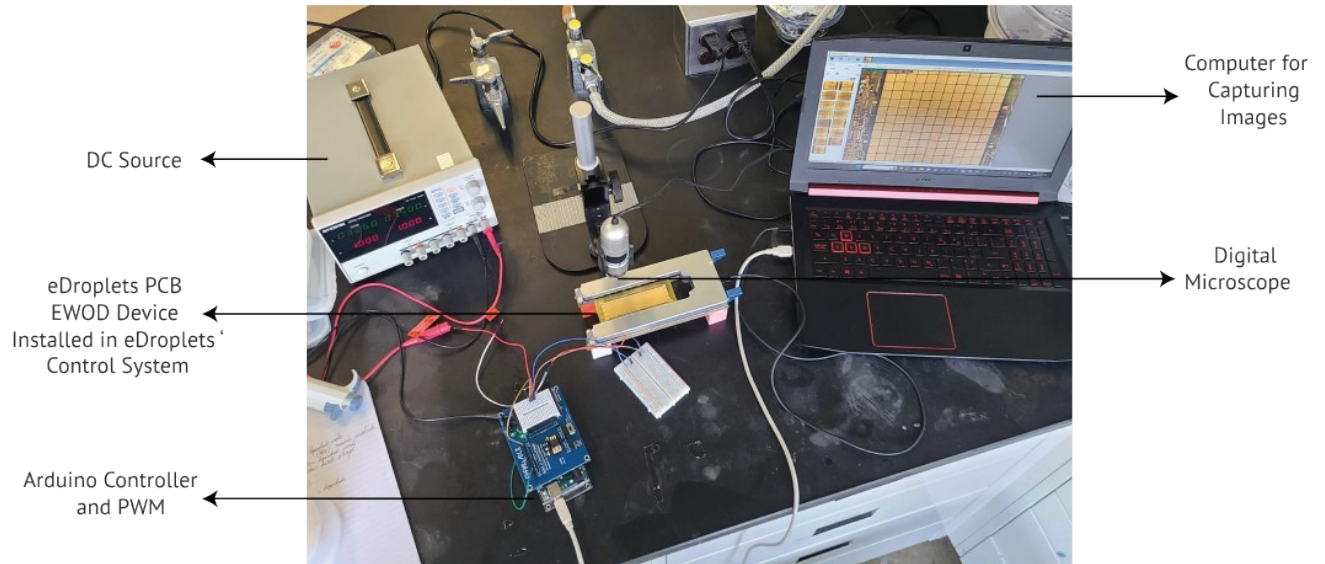


Figure S6: Experimental setup for performing the glucose assay via the *eDroplets* platform and thermal controller. The *eDroplets* platform and heater controller are connected to an external laptop with a user interface for droplet control. A microscope is mounted on top for droplet image acquisition.

## On-chip Glucose Assay Design

To prepare Fehling's solution, two components were freshly mixed: Fehling's A solution (diluted cupric sulphate) and Fehling's B solution, a mixture of sodium hydroxide and potassium tartrate, commonly referred to as Rochelle salt. Three concentrations of glucose solution (1.5%, 2% and 5% w/v) were prepared to optimize the reaction conditions. Upon heating the solutions to 70°C, the 1.5% w/v glucose solution exhibited a more pronounced color change, establishing this concentration as the primary choice for subsequent experiments.

## Heater and Sensor Layer Characterization

To address the heat conduction delay due to the FR4 layer (core layer), we initially employed the second copper layer as a heater, as shown in Fig. S7(b), and waited the EWOD surface to reach the desired temperature; the time ( $t_1$ ) was recorded. Then, the heater layer is changed to the third copper layer, and once again, the EWOD surface is waited to reach the temperature, and the time ( $t_2$ ) is recorded. The difference in these times results in a delay due to the core material, as the other layers, such as prepreg, are common between them in reaching the top surface.

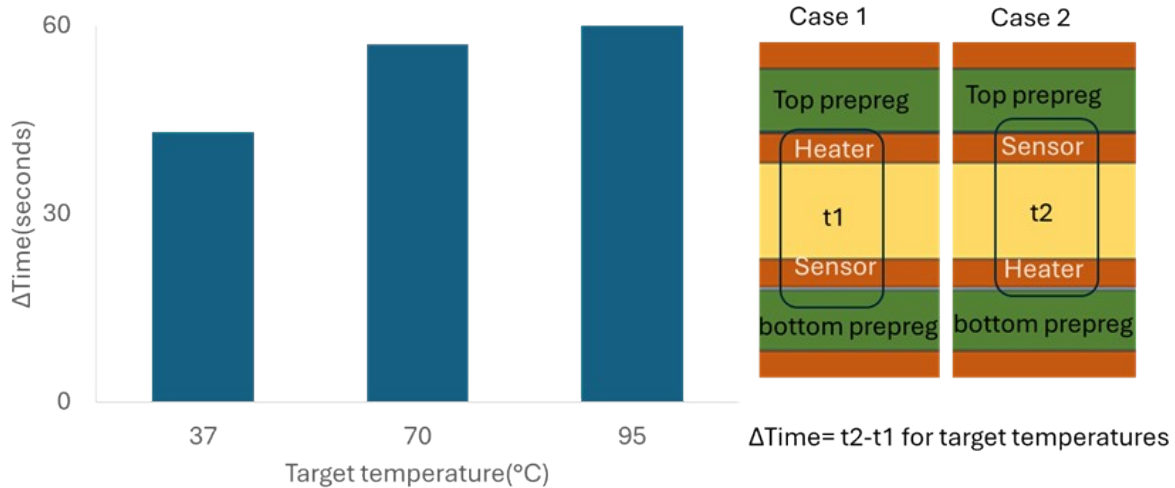


Figure S7: The figure (left) shows the time delay in reaching the target temperatures of 37, 70 and 95°C when the heater and sensor layers are interchanged. On the right are the heater and sensor positions, and t1 and t2 are the times taken to achieve the targeted temperatures.

Fig. S7(a) shows the delay time for the surface to reach temperatures of 37 °C, 70 °C, and 95 °C. Owing to the low thermal conductivity of the FR4 substrate, heat transfer was limited by its insulating properties. As a result, the thermal response time was the shortest for reaching 37 °C and progressively increased for higher target temperatures, with the longest delay observed at 95 °C. The heater layer, which is close to the top surface, was faster than the sensing layer, which is on the third copper layer of the printed circuit board stack-up (as shown in Figure S2).

The TrueIR Thermal Imager and its analysis tool were used to assess the temperature distribution on the EWOD electrodes with and without droplets on their surface. The results were analyzed to create the temperature distribution image displayed in Figure S8 =(a) & (b). Here, the heater surface was heated to approximately 70°C, and data were gathered for both the droplet-free and droplet-containing surfaces. As shown in Fig. S8(d), the data were plotted as a graph and smoothed down using the Savitzky-Golay method function. The temperature distributions of the surfaces with and without droplets are shown in the graph, with a difference of approximately 19 °C. Next, as shown in Fig. S8(e), we plotted the graph for the temperature distribution between the top and bottom of the droplet after running the simulation for the same heater temperature. As we can see, there was a variation of approximately 18 °C between the top and bottom. This demonstrates how the simulation and experiment closely match the vertical heat distribution inside the droplet. The vias in the model explain the dip in the middle of the droplet bottom temperature in the simulation results. The Thermal Imager cannot detect this phenomenon because it measures the emissivity of the surface value of the EWOD electrode.

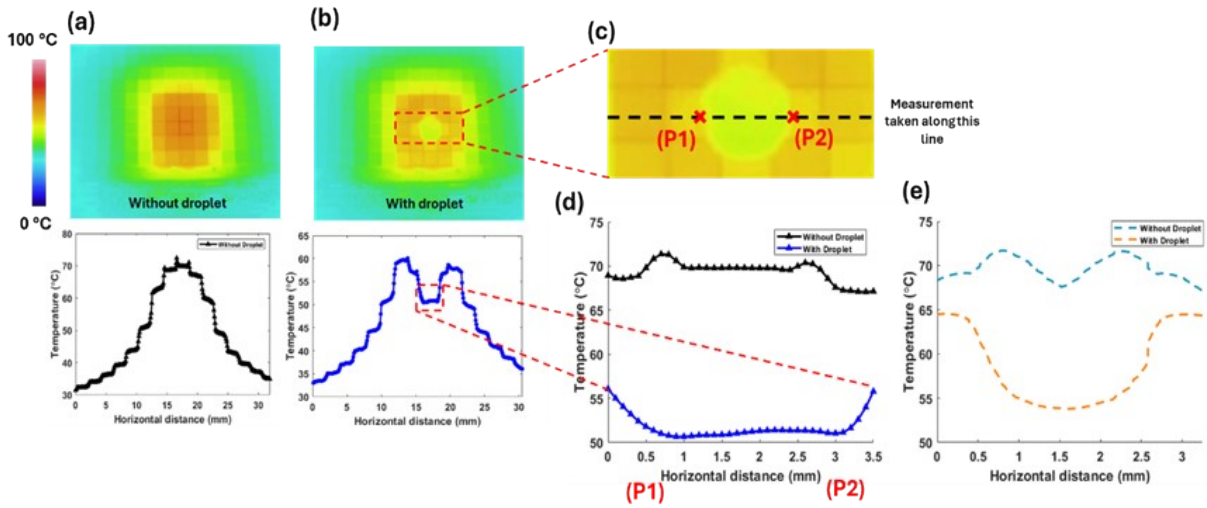


Figure S8: The temperature distribution of the EWOD surface: (a) The figure shows the top EWOD electrode heated to  $\sim 70^{\circ}\text{C}$  without a droplet, (b) with a droplet placed on EWOD with its temperature distribution along the line graph shown underneath it, (c) the zoomed-in image of the EWOD surface and the temperature distribution measured along the center line, (d) the graph shows the temperature distribution along the center line when there is no droplet and with a droplet, (e) graph shows the simulated results for the same amount of temperature actuated as seen in the previous graph temperature.

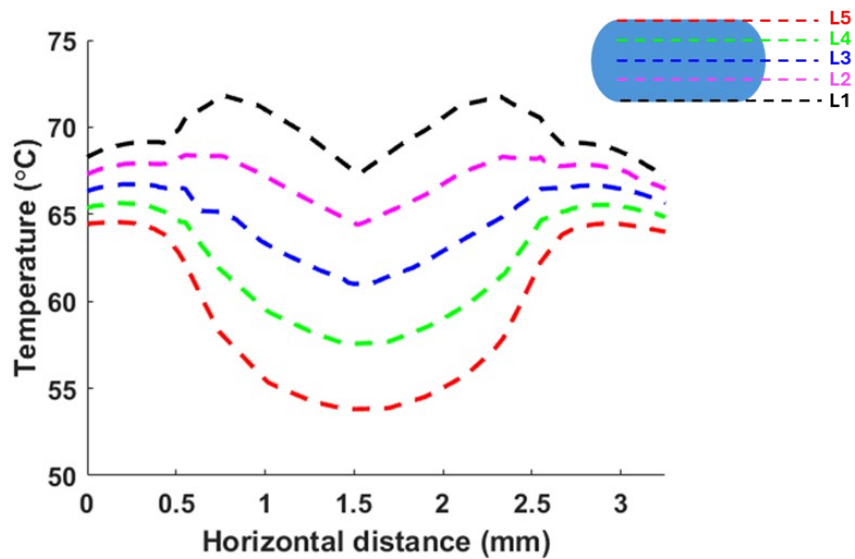


Figure S9: Numerical simulation results showing the temperature distribution inside the droplet for five various vertical heights from bottom to top on the basis of the results of the numerical simulation.